Low and variable pH decreases recruitment efficiency in populations of a temperate coral naturally present at a CO_2 vent

Erik Caroselli,[1] Francesca Gizzi,[1] Fiorella Prada,[1] Chiara Marchini,[1] Valentina Airi,[1] Jaap Kaandorp,[2] Giuseppe Falini,[3] Zvy Dubinsky,[4] Stefano Goffredo[1]*

[1]Marine Science Group, Department of Biological, Geological and Environmental Sciences, University of Bologna, Bologna, Italy
[2]Section Computational Science, University of Amsterdam, Amsterdam, The Netherlands
[3]Department of Chemistry "Giacomo Ciamician", University of Bologna, Bologna, Italy
[4]The Mina and Everard Goodman Faculty of Life Sciences, Bar Ilan University, Ramat Gan, Israel

Abstract

Atmospheric carbon dioxide enrichment alters seawater carbonate chemistry, thus threatening calcifying organisms such as corals. Coral populations at carbon dioxide vents are natural acidification experiments that mimic organism responses to seawater pH values projected for 2100. Even if demographic traits are paramount information to assess ecological relationships and habitat suitability, population dynamics studies on corals thriving under acidified conditions are lacking. Here, we investigate the demography and reproduction of populations of the solitary, symbiotic, temperate coral *Balanophyllia europaea* naturally living along a pH gradient at a Mediterranean CO_2 vent. Gametogenesis and larval production were unaffected while recruitment efficiency collapsed at low and variable pH, contributing to coral abundance decline and suggesting that life stages between larval release and early polyp growth are hindered by acidification. Exploring these processes is crucial to assess coral fate in the forthcoming acidified oceans, to preserve coral ecosystems and the socioeconomic services they provide.

The uptake of atmospheric carbon dioxide (CO_2) by ocean surface waters is reducing seawater pH and carbonate ion concentrations (Caldeira and Wickett 2003) with important consequences on calcifying marine organisms, including corals (Hoegh-Guldberg et al. 2017). Ocean acidity has increased of 25 30% (0.1 pH units) since the industrial revolution and a further increase by 150 200% is projected for the end of the century, equivalent to a drop by 0.3 pH units (Stocker et al. 2013).

The negative effects of ocean acidification on coral calcification, metabolism, survivorship, reproduction, and other fundamental processes have been investigated using laboratory and mesocosm experiments (Hoegh-Guldberg et al. 2017). These experiments are very important to investigate the response to short-term CO_2 partial pressure (pCO_2) increase, but they do not incorporate natural in situ conditions, organism adaptive capability, and organism experimental stress can bias acidification effects. Volcanic CO_2 vents can be used as natural laboratories to assess long-term ocean acidification impact on communities in a natural environment (Hall-Spencer et al. 2008; Fabricius et al. 2011; Baggini et al. 2014; Goffredo et al. 2014; Fantazzini et al. 2015; Linares et al. 2015; Gizzi et al. 2017; Prada et al. 2017). Many CO_2 vents present variations in temperature, salinity, total alkalinity, toxic gases, and metals, which can confound the effects of pCO_2 (Vizzini et al. 2013), but a few vents located in Italy (Hall-Spencer et al. 2008; Goffredo et al. 2014; Fantazzini et al. 2015; Gizzi et al. 2017; Prada et al. 2017), Papua-New Guinea (Fabricius et al. 2011), Greece (Baggini et al. 2014), and Japan (Inoue et al. 2013) have been used as natural laboratories for ocean acidification studies. These are exceptional research opportunities where organisms are naturally acclimated to ocean acidification. While having a similar mean to predicted changes in global acidity, pH conditions at CO_2 are usually variable and pH mean and variance are inversely correlated (Kerrison et al. 2011; Johnson et al. 2012). pH variance can significantly affect biological processes in different ways then changes in the mean (Dufault et al. 2012; Johnson et al. 2014), and since mean and variance cannot be separated at these sites, they do not perfectly match climate change-induced acidification (Johnson et al. 2012). Nevertheless, these vents can

*Correspondence: s.goffredo@unibo.it

Author Contribution Statement: EC, FG, FP, and SG performed the fieldwork; EC, FG, FP, CM, VA, JK, and SG performed the analyses; EC, FG, FP, CM, VA, GF, and SG wrote the manuscript. GF, ZD, and SG conceived the experiments. All authors participated to the scientific discussion.

Additional Supporting Information may be found in the online version of this article.

provide indications about future ocean acidification consequences on calcifying organisms, based on what is already observed on native molluscs and corals, which become less abundant (Hall-Spencer et al. 2008; Fabricius et al. 2011; Goffredo et al. 2014), calcify less, and dissolve their carbonate structures (Hall-Spencer et al. 2008; Rodolfo-Metalpa et al. 2011; Goffredo et al. 2014; Fantazzini et al. 2015).

Population demographic analyses are important to reveal relationships between organisms and their environment (Bak and Meesters 1998; Goffredo et al. 2008, 2010; Caroselli et al. 2016, 2017) and assess population turnover. This can be useful for restoration actions (Knittweis et al. 2009), yet no information on ocean acidification effects on the dynamics of coral populations naturally thriving in acidified seawater is currently available. Similarly, there is no information from field studies on ocean acidification effects on reproduction of corals. Experiments in controlled conditions and simulation models suggest that a compromised gamete production, sperm motility (Morita et al. 2009; Nakamura et al. 2011), gametogenesis (Jokiel et al. 2008), fertilization (Albright et al. 2010; Albright and Mason 2013), embryo development (Medina-Rosas et al. 2012), larval settlement, and juvenile growth (Albright et al. 2008; Albright and Langdon 2011; Nakamura et al. 2011; Doropoulos et al. 2012) can occur under acidified conditions, all of which could impact population dynamics (Bramanti et al. 2015).

Here, we describe, for the first time, the effect of low and variable pH on population dynamics and recruitment efficiency of the temperate, symbiotic, solitary coral *Balanophyllia europaea* (Risso, 1826), naturally living along a natural pCO_2 gradient close to Panarea Island (Italy). The shallow depth and the lack of heated or toxic compounds (Goffredo et al. 2014) give an opportunity to investigate the influence of ocean acidification on marine organisms, including *B. europaea*. Populations of this simultaneous hermaphrodite and brooding coral (Goffredo et al. 2002) naturally growing along the pCO_2 gradient are less abundant and decrease their net calcification rate with decreasing pH, while preserving their linear extension rate at the expense of skeletal bulk density, which strongly decreases (Goffredo et al. 2014; Fantazzini et al. 2015). Coral skeletons of *B. europaea* become more porous and less resistant to breakage as pH decreases, while nanoscale properties of calcium carbonate crystals are preserved (Fantazzini et al. 2015). Short-term transplant experiments have revealed increased mortality of this species at lower and variable pH, but a stable net calcification even under extreme pH levels, probably due to the short experimental exposure to acidified conditions (3 months) (Prada et al. 2017). Given the observed homogeneous linear extension rate with increasing acidification (Fantazzini et al. 2015), we expected to find no effects on age/-length relationships, nor on the functional sexual reproductive cycle. It has been hypothesized that energy may be allocated to the linear extension rate in order to reach sexual maturity size (Fantazzini et al. 2015).

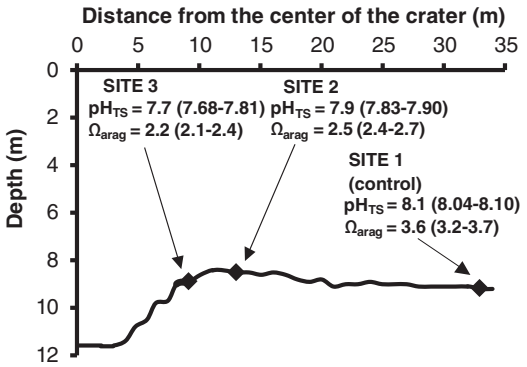

Fig. 1. Bathymetric profile along the pH gradient, with the position, mean pH_{TS}, and Ω_{arag} of the three sampling sites. 95% confidence interval in brackets.

Materials and methods

Study site and sample collection

This observational study was performed close to Panarea (Italy), an island of the Aeolian Archipelago (Italy) that is part of an active volcanic system characterized by a widespread presence of gas vents and hot water springs with different geochemical characteristics (Gamberi et al. 1997; De Astis et al. 2003; Tassi et al. 2009). Among them, close to the Bottaro rock, a crater (20 × 14 m) at ~ 10 m depth emits a stable column of bubbles (98 99% CO_2) at ambient temperature, without toxic compounds such as metals and H_2S, thus generating a natural pH gradient extending for ~ 34 m (Capaccioni et al. 2007; Goffredo et al. 2014; Fantazzini et al. 2015). Three sampling sites whose seawater physic-chemical parameters have been previously characterized (Goffredo et al. 2014; Fantazzini et al. 2015; Prada et al. 2017) were selected along the gradient (Fig. 1). Site 1 (pH total scale [pH_{TS}] = 8.1; 95% confidence intervals [CI] = 8.04 8.10) was used as control, site 2 (pH_{TS} = 7.9; 95% CI = 7.83 7.90) aligns with IPCC's mean pH prediction of a conservative CO_2 emissions scenario (Representative Concentration Pathway, RCP6.0), and site 3 (pH_{TS} = 7.7; 95% CI = 7.68 7.81) fits the "business-as-usual" CO_2 emissions scenario (RCP8.5). No coral was present between site 3 and the center of the crater, at lower pH_{TS} (Goffredo et al. 2014; Fantazzini et al. 2015).

In order to test the effects of low and variable pH on coral growth, on 09 March 2011 and 04 November 2012, 10 11 random specimens of *B. europaea* were collected from sites 1 3 using a hammer and chisel. Sample size was determined based on previous studies on the species, where a similar sample size allowed to reliably characterize biometry and growth. Samples were dried, cleaned, and polyp length (*L*: maximum axis of the oral disk) and dry skeletal mass (*M*) determined with standard protocols (Goffredo et al. 2007, 2010; Caroselli et al. 2017).

On 28th April 2013, an additional sampling was performed to collect 10 specimens of *B. europaea* from sites 1 3 for reproductive analyses. In this period, the annual reproductive cycle presented maximum gonadal development (before fertilization), characterized by two stocks of oocytes, a small one (< 300 μm, immature oocytes) that will be fertilized in the following reproductive year, and a large one (> 300 μm; mature oocytes) that will be fertilized in the same reproductive year (Goffredo et al. 2002; Airi et al. 2014). Only sexually mature individuals (length > 6 mm) were collected to limit the impact on the natural population, whose abundance significantly decreased with acidification along the pH gradient (Fantazzini et al. 2015). Polyp length, width (W: minimum axis of the oral disk), and height (h: oral-aboral axis) were measured with calipers (Goffredo et al. 2007, 2008; Caroselli et al. 2016). Skeletal volume was estimated with the formula $V = \frac{L}{2} \times \frac{W}{2} \times h\pi$ (Goffredo et al. 2002, 2007, 2008; Caroselli et al. 2015, 2017). Polyps were fixed in saturated formalin solution (10% formaldehyde and 90% seawater; the solution was saturated with calcium carbonate) and transferred to the laboratories for cyto-histometric analyses (Airi et al. 2014; Gizzi et al. 2017; and references therein).

Growth modeling

By means of computerized tomography (CT; CT scanner type = Philips Brilliance CT 64; slice thickness = 0.7 mm; MTF 0 spatial resolution = 24 line pairs cm^{-1}), the number of annual growth bands of collected samples was counted to obtain their age using the software Philips e-Film 1.5.3 (Goffredo et al. 2008; Fantazzini et al. 2015). Growth was modeled on the von Bertalanffy growth function, which has been previously validated for populations of *B. europaea* across its latitudinal range (Goffredo et al. 2008) and whose assumptions were checked and met at all sites (mean growth rate decreased exponentially with age; Fig. 2B):

$$L_t = L_\infty \left(1 - e^{-kt}\right) \quad (1)$$

where L_t is individual length at age t, L_∞ is the asymptotic length (maximum expected length in the population), k is a growth constant (larger for fast growth up to the asymptotic length, smaller for slow growth), and t is the age of the individual. L_∞ and k, along with their CI, were estimated for each site through a regression analysis by least squares procedure developed in the software MATLAB R2012a (MathWorks, Natick, U.S.A.) (Caroselli et al. 2016, 2017).

Photoquadrats

From July 2011 to April 2013, specimens of *B. europaea* present inside haphazardly placed 0.25 m^2 PVC quadrats at sites 1 3 were photographed underwater using a Canon G11 (26 33 quadrats per site) during four expeditions. The number of quadrats was determined by balancing the need for sufficient replicates to represent the population structure but without moving to far from the center of the site, where environmental parameters were measured (i.e., moving too far from the center of each site would have provided data about corals subject to different environmental parameters than those characterizing the site). Pictures were analyzed with the software NIKON NIS-Elements D 3.2 to count individuals and measure their L. Their M was estimated by applying to their L the M/L relationship of collected samples. Population

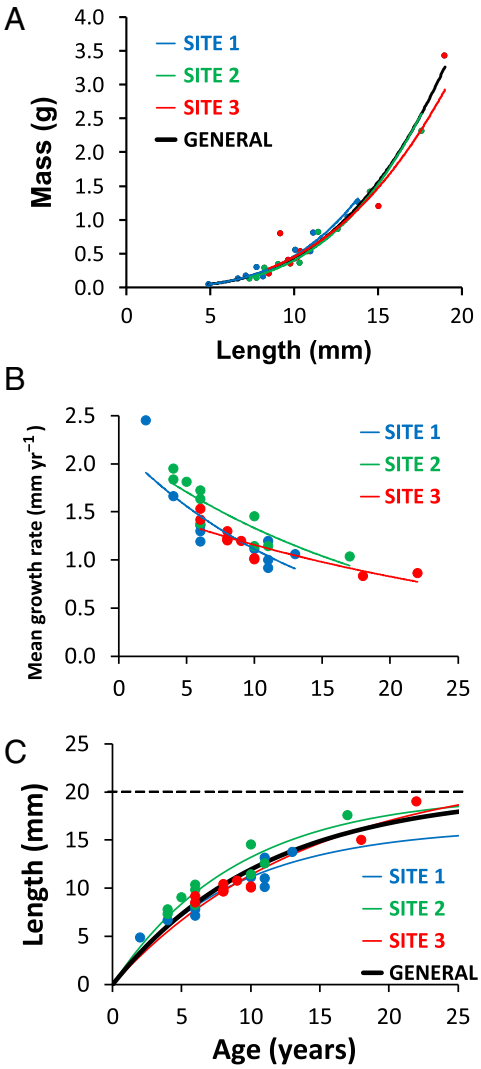

Fig. 2. Biometry and growth. (**A**) Mass length relationship in the three sites, and general relationship across sites. Site 1: N (number of individuals) = 10, $y = 0.0003\ x^{3.241}$, R^2 (Pearson's determination coefficient) = 0.961, p (significance of the correlation) < 0.001; site 2: $N = 10$, $y = 0.0002\ x^{3.277}$, $R^2 = 0.960$, $p < 0.001$; site 3: $N = 11$, $y = 0.0006\ x^{2.909}$, $R^2 = 0.839$, $p < 0.001$; General: $N = 31$, $y = 0.0003\ x^{3.138}$, $R^2 = 0.932$, $p < 0.001$. (**B**) Relationships between mean growth rate and age at each site. Site 1: $N = 10$, $R^2 = 0.749$, $p < 0.010$; site 2: $N = 10$, $R^2 = 0.800$, $p < 0.001$; site 3: $N = 11$, $R^2 = 0.780$, $p < 0.001$. (**C**) Age length von Bertalanffy growth curves for each site. Dotted line indicates the maximum expected length of corals in all populations (L_∞ = 20.0 mm). Points indicate the age/size of samples dated by CT scans. N = number of individuals dated by CT scans. [Color figure can be viewed at wileyonlinelibrary.com]

density was estimated as NI (number of individuals m^{-2}) and MA (mass per m^{-2}) (Goffredo et al. 2007). Size structure of each site was derived by these photoquadrat measurements.

Demography

The von Bertalanffy age-length relationship (Eq. 1) was used to estimate the age of all samples in photoquadrats, thus obtaining a population age structure of each site from the corresponding size structure. The mean age of individuals at each site was computed from the age of samples in photoquadrats dated with the growth curve (Eq. 1). The percentage of individuals below sexual maturity was obtained by summing the frequencies of the age classes below sexual maturity, which is ~ 5 yr (~ 6 mm length) (Goffredo et al. 2002). The biomass distribution per age class was obtained by the sum of each corallite *M* in each age class. The age at maximum percentage biomass was determined as the age class containing the mode of percentage biomass. The mean age of biomass in the populations was calculated as the sum of the products of the observed biomass in each age class multiplied by its age, then divided by the total biomass.

Cyto-histometric analysis

Polyps collected for reproductive analyses were postfixed in Bouin solution. After decalcification in EDTA and dehydration in a graded alcohol series from 80% to 100%, polyps were embedded in paraffin, and serial transverse sections were cut at 7 μm intervals from the oral to the aboral poles. Tissues were stained with Mayer's hematoxylin and eosin (Goffredo et al. 2002). Cytometric analyses were performed with a light microscope NIKON Eclipse 80i using an image analysis system: NIKON NIS-Elements D 3.1. Oocytes and spermaries were classified into developmental stages (Goffredo et al. 2002).

Reproductive parameters

Reproductive output was defined through three parameters: (1) oocyte and (2) spermary abundance, both defined as the number of reproductive elements per unit body volume (100 mm^3); (3) fertility, defined as the number of mature oocytes per unit body volume (100 mm^3), assuming each mature oocyte will result in a larva (planula) (Goffredo et al. 2010); and (4) gonadal index, defined as the percentage of body volume occupied by oocytes and spermaries.

Life table

A static life history table was produced for each of the three sites where corals were collected. Size at sexual maturity and percentage of mature polyps in each age class were derived from previous reproductive studies on *B. europaea* (Goffredo et al. 2002; Airi et al. 2014). The number of planulae released by each age class (biXi) was estimated by multiplying: fertility (bi), number of individuals (Xi), and percentage of mature polyps (Fi) (Goffredo et al. 2010; Caroselli et al. 2017).

Statistical analysis

Levene's test was used to test homogeneity of variance. Kolmogorov Smirnov was used to test normality of data distributions and differences in age frequency distributions among the three sites. Kruskal-Wallis test was used as a robust non-parametric alternative to the ANOVA for data that did not assume normal distributions and was used to test differences in mean population density (NI and MA) and reproductive parameters (oocyte and spermary abundance, and gonadal index) among the three sites. Analyses were performed using the software SPSS Statistic 22.0 (IBM).

A one-way permutation multivariate analysis of variance (PERMANOVA) (Anderson 2005) based on Euclidean distances was performed to test differences in oocyte distribution and spermary maturation stage distribution among sites, using the software Primer 6 (Quest Research Limited).

Results

Coral growth patterns

Analyses were performed on *B. europaea* samples collected along the Panarea pCO_2 gradient at three sites (pH_{TS} range 8.1 7.7; Fig. 1), whose seawater carbonate chemistry has been characterized in detail (Goffredo et al. 2014; Fantazzini et al. 2015; Prada et al. 2017). Polyp length was selected as the main biometric parameter because it was the most highly correlated with skeletal mass and it has been used in previous analyses on this species and other solitary corals (Goffredo et al. 2007, 2008, 2010; Caroselli et al. 2016, 2017). The exponents and scaling factors of power function relationships between mass and length (Fig. 2A) were homogeneous among sites (95% CI were overlapped), thus data were pooled to obtain a general relationship across all sites (Fig. 2A; Table 1).

At each site, coral growth decreased exponentially with age, which explained 75 80% of mean growth rate variation (Fig. 2B). This typical growth pattern is characteristic of *B. europaea* (Goffredo et al. 2008) and other solitary corals (Goffredo et al. 2010; Caroselli et al. 2016). The asymptotic maximum length (L_∞) and the growth constant (k) of age-length growth curves at each site were homogeneous (95% CI overlapped; Table 1). Therefore, data were pooled to estimate L_∞ and k (Table 1) of the general growth curve describing the age-length relationship across all sites (Fig. 2C) and allowing age determination of all samples in photoquadrats from the three sites.

Population demographic traits

The abundance of individuals and biomass per surface area decreased at lower and variable pH_{TS} (number of individuals m^{-2} decreased by 86% between mean pH_{TS} 8.1 and 7.7; Kruskal-Wallis test, $p = 4 \times 10^{-4}$; mass per m^{-2} decreased by 64% between mean pH_{TS} 8.1 and 7.7; Kruskal-Wallis test, $p = 7 \times 10^{-8}$; Table 2).

Photoquadrats enabled the measurement of the length of 180 individuals that were dated using the general age-length

Table 1. Mean pH_{TS}, number of collected corals, mass/length and length/age relationship parameters, and mean age at each site. Ranges in brackets are 95% CI.

	Site 1	Site 2	Site 3	General
Annual mean pH_{TS}	8.1	7.9	7.7	
Number of corals	10	10	11	31
M/*L* relationship exponent	3.241 (2.706 3.776)	3.277 (2.730 3.824)	2.909 (1.949 3.869)	3.138 (2.815 3.461)
M/*L* relationship scaling factor	0.0003 (0.0001 0.0009)	0.0002 (0.0001 0.0008)	0.0006 (0.0001 0.0055)	0.0003 (0.0001 0.0007)
L_∞ (mm)	16.4 (9.1 23.8)	19.7 (14.0 25.5)	22.6 (16.5 28.7)	20.0 (16.1 24.0)
k (yr^{-1})	0.115 (0.023 0.206)	0.111 (0.055 0.167)	0.070 (0.041 0.100)	0.091 (0.061 0.121)
Mean age (yr)	8.0 (5.7 10.3)	7.9 (5.4 10.4)	10.3 (7.3 13.3)	8.8 (7.2 10.3)

M, mass; *L*, length; L_∞, asymptotic length; *k*, growth constant.

growth curve (Fig. 2C). The oldest individual was observed at mean pH_{TS} 7.7 with an estimated age of 16 yr and a length of 15.3 mm. Age-frequency distributions (Fig. 3) differed among sites (Kolmogorov Smirnov test, $p = 0.004$ for mean pH_{TS} 8.1 vs. 7.9, $p = 0.009$ for mean pH_{TS} 8.1 vs. 7.7, $p = 0.959$ for mean pH_{TS} 7.9 vs. 7.7) and all derived demographic parameters ranked according to mean pH_{TS} (Table 2, Fig. 3). The percentage of immature individuals decreased (from 47.7% at mean pH_{TS} 8.1 to 20.0% at mean pH_{TS} 7.7) at lower and variable pH_{TS}, while the mean age (from 5.6 yr at mean pH_{TS} 8.1 to 9.4 yr at mean pH_{TS} 7.7), age at maximum percentage biomass (from 6 yr at mean pH_{TS} 8.1 to 14 yr at mean pH_{TS} 7.7), and mean age of biomass (from 7.7 yr at mean pH_{TS} 8.1 to 11.5 yr at mean pH_{TS} 8.1) increased at lower and variable pH_{TS} (Table 2; Fig. 3).

Quantification of sexual reproduction

The distribution and morphology of both female and male germ cell maturation stages were homogeneous among sites (PERMANOVA; $p = 0.139$ for spermary size class distributions; $p = 0.186$ for spermary maturation stages; $p = 0.115$ for oocyte size class distributions; Fig. 4 and Supporting Information Fig. S1). Corals were all hermaphrodites with two distinct stocks of small (immature, $< 300\ \mu m$) and large (mature, $> 300\ \mu m$) oocytes and with spermaries at both early and advanced maturation stages (Fig. 4 and Supporting Information Fig. S1). Oocyte and spermary abundance and gonadal index, and fertility were not correlated with mean pH_{TS} (Supporting Information Tables S1, S2 and Fig. S2).

Insights on recruitment efficiency

Based on the observed populations, during 1 yr polyps released 2074 larvae m^{-2} at mean pH_{TS} 8.1, 1479 larvae m^{-2} at mean pH_{TS} 7.9, and 953 larvae m^{-2} at mean pH_{TS} 7.7 (Supporting Information Table S3). Assuming local recruitment (Goffredo et al. 2004), the individuals : larvae ratio decreased with at lower and variable pH from 1 : 93 at mean pH_{TS} 8.1 to 1 : 338 at mean pH_{TS} 7.7 (Table 2 and Supporting Information Table S3). The same trend was observed by

Table 2. Mean annual pH_{TS}, number of patches (photoquadrats) and individuals, and demographic parameters at each site. Ranges in brackets are 95% CI.

	Site 1	Site 2	Site 3
pH_{TS}	8.1	7.9	7.7
Number of patches	33	29	26
Number of observed samples	128	37	15
Number of individuals m^{-2} (NI)	22 (12 33)	7 (3 11)	3 (0 6)
Mass per m^{-2} (MA)	5.6 (2.4 8.8)	3.1 (0.5 5.7)	2.0 (0.5 3.5)
% of immature individuals	47.7	32.4	20.0
Mean age (yr)	5.6	7.5	9.4
Age at max % biomass (yr)	6	8	14
Mean age of biomass (yr)	7.7	10.2	11.5
Larval production (planulae m^{-2})	2074 (1424 2729)	1479 (1016 1941)	953 (660 1244)
Mean individuals : planulae ratio	1 : 93	1 : 218	1 : 338
	1 : (63 122)	1 : (150 287)	1 : (234 441)
Mean immature individuals : planulae ratio	1 : 195	1 : 673	1 : 1690
	1 : (134 257)	1 : (463 884)	1 : (1171 2206)
Mean mature individuals : planulae ratio	1 : 178	1 : 323	1 : 423
	1 : (122 234)	1 : (222 424)	1 : (293 552)

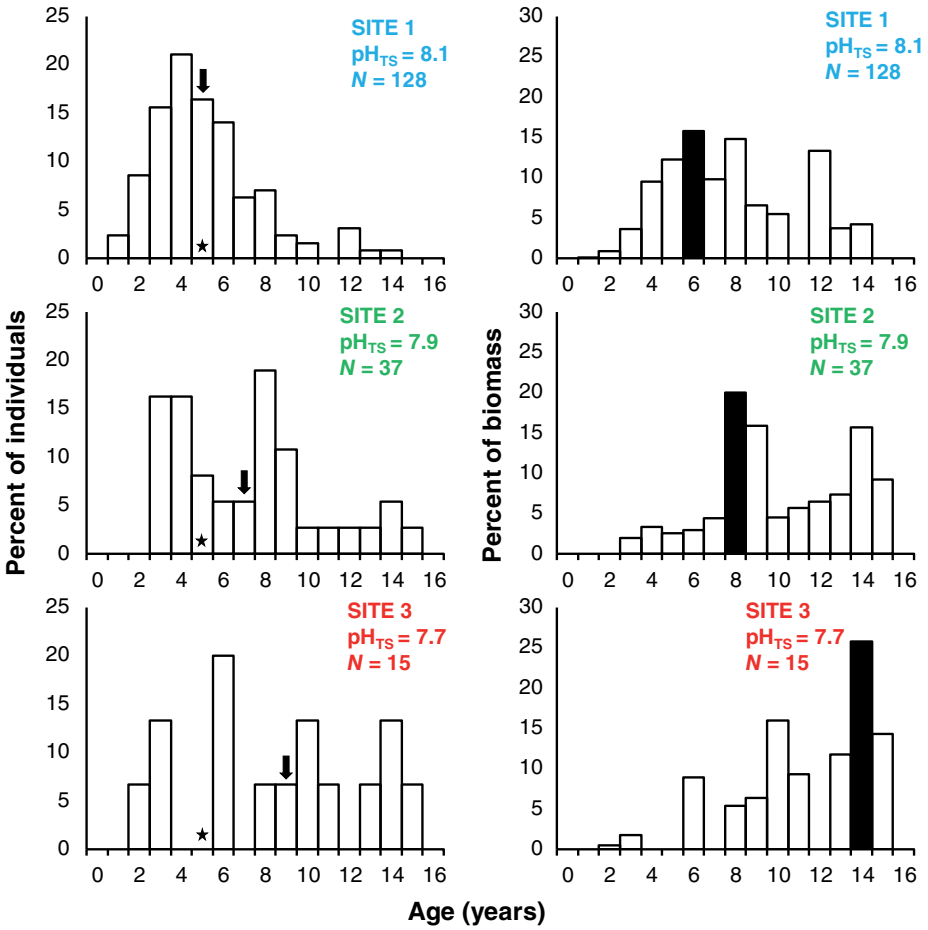

Fig. 3. Age class structure by abundance and percentage of biomass at the three sites. The age class containing the mean age of the individuals (black arrow) and the age at maximum percentage biomass (black column) are indicated. Stars indicate the age at sexual maturity. [Color figure can be viewed at wileyonlinelibrary.com]

analyzing only the fractions of sexually immature (immature individuals : larvae ratio decreased from 1 : 195 at mean pH_{TS} 8.1 to 1 : 1690 at mean pH_{TS} 7.7) and mature individuals (mature individuals : larvae ratio decreased from 1 : 178 at mean pH_{TS} 8.1 to 1 : 423 at mean pH_{TS} 7.7; Table 2 and Supporting Information Table S3).

Discussion

Population demographic traits

The decrease in abundance of individuals (NI decreased by 86% between mean pH_{TS} 8.1 and 7.7; Kruskal-Wallis test, $p = 4 \times 10^{-4}$; Table 2) and biomass per surface area (MA decreased by 64% between mean pH_{TS} 8.1 and 7.7; Kruskal-Wallis test, $p = 7 \times 10^{-8}$; Table 2) at lower and variable pH agrees with the observed decrease in *B. europaea* percent cover along this gradient (Goffredo et al. 2014). Observed demographic trends reveal a pattern of progressive deficiency of young, immature individuals at lower and variable pH, and an associated increase in mean age of populations. The same pattern is reported also in *B. europaea* populations subjected to increasing high-temperature stress along a wide latitudinal gradient on Italian coasts (Goffredo et al. 2008). Along the temperature gradient, the deficit of young individuals is linked to a decrease of symbiont photosynthesis at high temperatures (Caroselli et al. 2015) and the consequent decrease of energetic resources available to the coral (Goffredo et al. 2014). In our case, symbiont photosynthesis is expected to be unaffected or even increase in acidified conditions, due to increased availability of CO_2 (Brading et al. 2011), thus it is unlikely to be related to the observed deficit of immature corals at lower pH_{TS}. Therefore, we investigated possible variations of reproductive efficiency of *B. europaea* at lower and variable pH_{TS}.

Quantification of sexual reproduction

With increasing acidification, *B. europaea* is reported to drop the net calcification rate and deposit less dense and more porous (i.e., more fragile) skeletons, while linear extension rate is maintained, probably to allow reaching the size at sexual maturity and reproduce even in acidified stressful conditions (Fantazzini et al. 2015). The above hypothesis is confirmed by our results on reproductive parameters. In fact, at all sites,

both male and female gametogenesis followed the typical reproductive pattern and timing of *B. europaea* (Goffredo et al. 2002), without differences associated to pH_{TS}. This result is in agreement with the findings of a recent study conducted at the same CO_2 vent on a non-zooxanthellate coral species and with previous analyses in mesocosms and aquarium conditions that reported a normal gametogenesis under acidified conditions (Jokiel et al. 2008; Gizzi et al. 2017). Thus, also gametogenesis is not the cause of the observed decrease of population density of *B. europaea* with decreasing pH_{TS} (Goffredo et al. 2014).

Insights on recruitment efficiency

Even if polyp reproduction was unaffected, the incorporation of demographic data revealed a strong decrease of larval production at lower and variable pH_{TS}, caused by the decreasing abundance of individuals. Also, recruitment efficiency strongly decreased at lower and variable pH_{TS}, because more larvae were required to obtain one settled polyp. It has to be noted that our estimation of recruitment efficiency assumed closed populations, while it may be possible that larvae come in from the outsides of our study sites (i.e., populations may be open). Unfortunately, there is no information on larval dispersal of this species in nature, even if population genetics studies suggest that populations separated on the spatial scale of tens of meters are relatively separated (Goffredo et al. 2004). Nevertheless, even if a certain number of larvae reach the three study sites from other nearby sites, this influx would affect our life table by slightly increasing the estimated larval mortality at each site. However, the general trend of decreasing recruitment efficiency with acidification would still remain, unless a disproportioned amount of larvae from outside reached the control and not the acidified sites (which is unlikely or at least there is no evidence that suggests it).

The observed decrease in recruitment efficiency indicates that some biologic process between larval production and the growth of the young polyp (i.e., planulation success, larval free-living stage, larval settlement, metamorphosis, and early skeletogenesis) is likely hindered at lower and variable pH_{TS}. In the present study, mature oocytes were assumed to result in one larvae, but processes of egg fertilization and embryo development may also be affected by acidification and contribute to the observed decrease of recruitment efficiency. Indeed, aquarium experiments on tropical corals have reported that

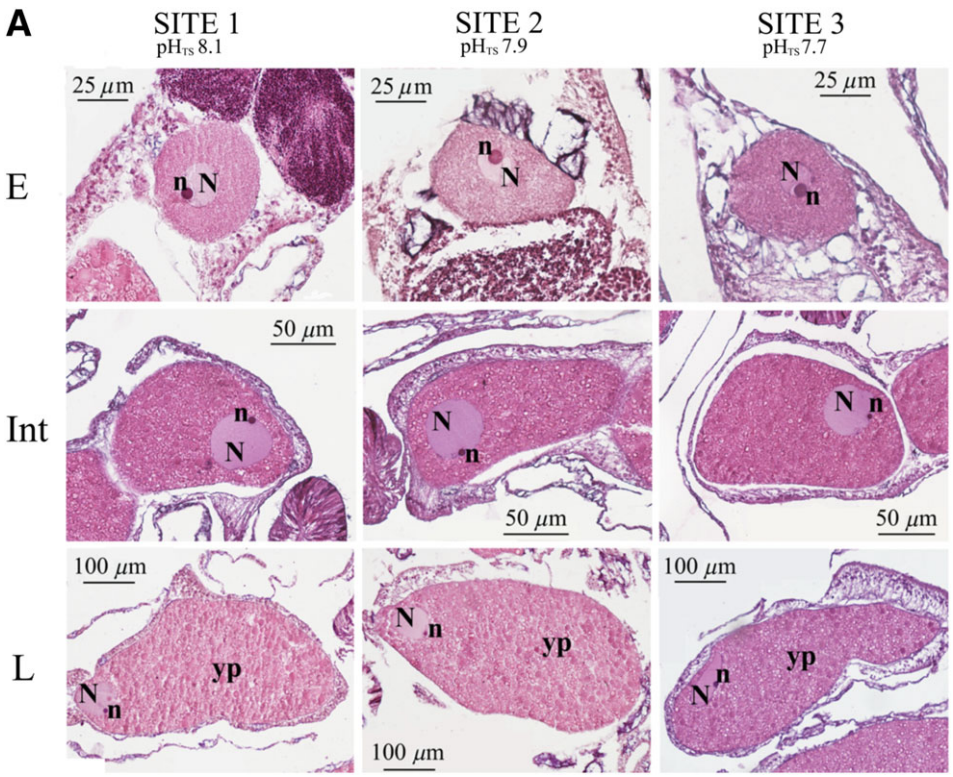

Fig. 4. Gametogenesis. (**A**) Three stages of oogenesis. E = early stage: Small oocyte with high nucleus : cytoplasm ratio and the spherical central nucleus (*N*) that contains the nucleolus (n). Int = intermediate stage: Medium sized oocyte with quite homogeneous cytoplasm; nucleus has started to migrate toward cell periphery. L = late stage: Small yolk plates (yp) fill the ooplasm; nucleus reached cell periphery. (**B**) Five stages of spermatogenesis. I: undifferentiated germ cells (spermatogonia, sg) in the gastrodermis (g). II: spermatocytes (sc) undergoing meiosis compose the spermary. III: spermaries delineated by a wall arisen from the mesoglea (arrows). IV: spermary with an external layer of spermatocytes and an internal mass of spermatids (st). V: spermary made of spermatozoa (sz). [Color figure can be viewed at wileyonlinelibrary.com]

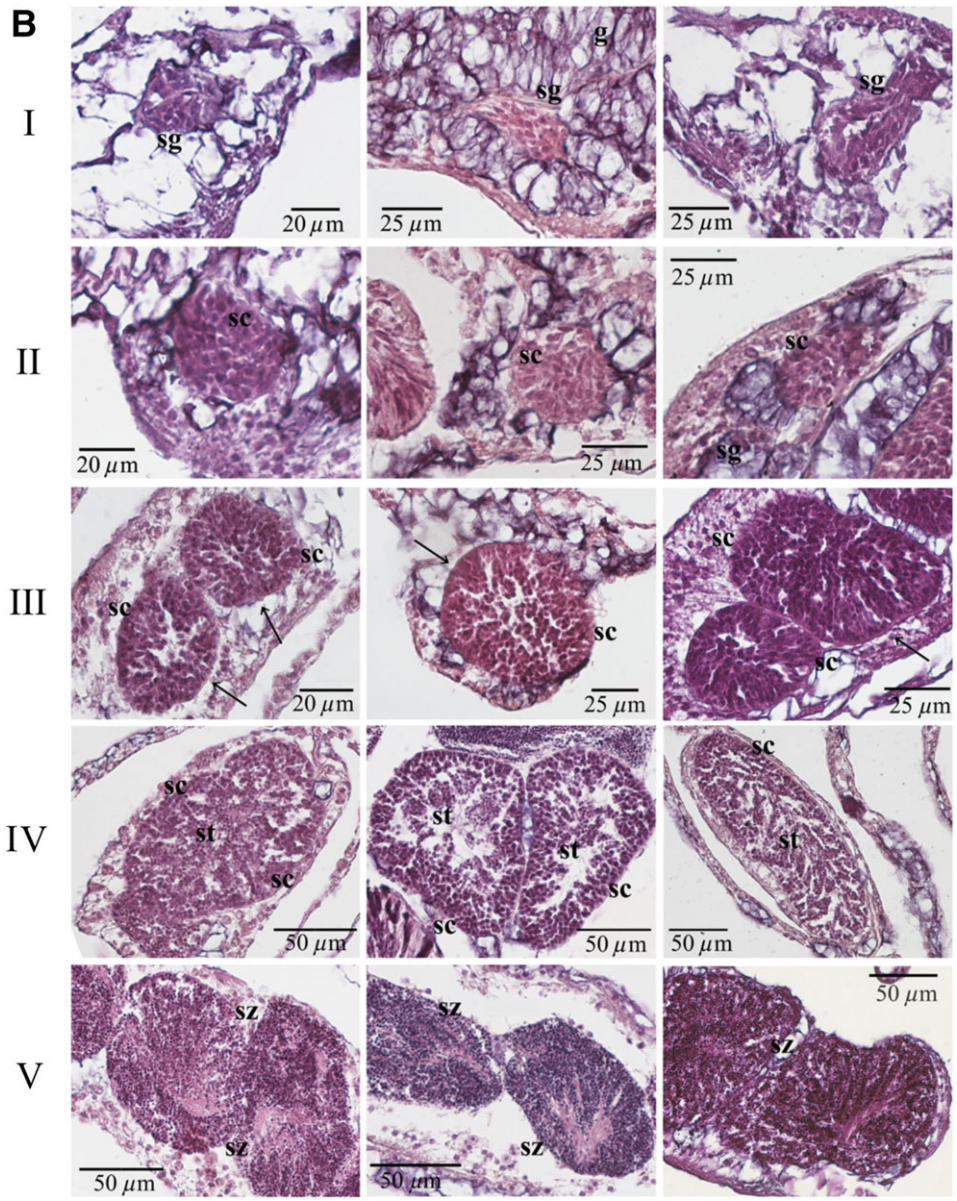

Fig. 4. Continued.

acidification reduces sperm motility (Morita et al. 2009; Nakamura and Morita 2012) and impairs larval metabolism, metamorphosis, and settlement (Albright et al. 2010; Albright 2011; Albright and Langdon 2011; Doropoulus 2012; Albright and Mason 2013; Webster et al. 2013). Moreover, a recent study conducted at CO_2 vents in Papua New Guinea showed that ocean acidification lowers the recruitment of corals that are naturally thriving under low pH by hindering the life stages between larval release and early polyp growth (Fabricius et al. 2017). Alternatively, or in addition to, the direct effect of mean pH and its variability, other potential cofactors could influence our observations. Acidification effects acting on other components of the local physical and biological habitat could be responsible, or contribute to, the decrease in recruitment efficiency of *B. europaea*. For example, site 1 is a typical healthy Mediterranean rocky habitat with *Posidonia oceanica*, while in sites 2 and 3 *Posidonia* is not present and composition of macroalgal species varies along the gradient (Goffredo et al. 2014), and the dynamics of coral larval settlement may consequently be altered.

Conclusions

We document here the first analysis of reproduction and population dynamics of coral populations naturally present along a CO_2-driven seawater acidification spatial gradient.

Lower and variable pH conditions reduce calcification and skeletal density and resistance, while linear extension is preserved (Fantazzini et al. 2015) to reach size at sexual maturity and reproduce. In fact, larval production, estimated from mature oocytes, resulted unaffected. However, the fraction of young individuals and recruitment efficiency strongly decrease at lower and variable pH_{TS}, in agreement with the observed decrease in population abundance. This seems a general stress response of this species, because the same responses are observed along a wide latitudinal gradient of increasing temperature (Goffredo et al. 2007, 2008, 2009; Airi et al. 2014). Early life stages between larval production and recruit growth are proposed here as coral Achilles' heel in an acidifying and warming ocean. Investigating these processes in coral populations naturally acclimated to ocean acidification and warming is required to clarify how the forthcoming seawater conditions will impact coral life history traits and the related ecosystem services they provide to human society. In addition to ocean acidification and warming, also other stressors such as eutrophication are likely to exacerbate the negative effects of increased carbon dioxide on marine ecosystems (Kroeker et al. 2013). Replication of studies like the one presented here in a wider range of settings would help to predict how different species will respond to future environmental conditions.

References

Airi, V., F. Gizzi, G. Falini, O. Levy, Z. Dubinsky, and S. Goffredo. 2014. Reproductive efficiency of a Mediterranean endemic zooxanthellate coral decreases with increasing temperature along a wide latitudinal gradient. PLoS One **9**: e91792. doi:10.1371/journal.pone.0091792

Albright, R. 2011. Reviewing the effects of ocean acidification on sexual reproduction and early life history stages of reef-building corals. J. Mar. Biol. **2011**: 1 14. doi:10.1155/2011/473615

Albright, R., B. Mason, and C. Langdon. 2008. Effect of aragonite saturation state on settlement and post-settlement growth of *Porites astreoides* larvae. Coral Reefs **27**: 485 490. doi:10.1007/s00338-008-0392-5

Albright, R., B. Mason, M. Miller, and C. Langdon. 2010. Ocean acidification compromises recruitment success of the threatened Caribbean coral *Acropora palmata*. Proc. Natl. Acad. Sci. USA **107**: 20400 20404. doi:10.1073/pnas.1007273107

Albright, R., and C. Langdon. 2011. Ocean acidification impacts multiple early life history processes of the Caribbean coral *Porites astreoides*. Glob. Chang. Biol. **17**: 2478 2487. doi:10.1111/j.1365-2486.2011.02404.x

Albright, R., and B. Mason. 2013. Projected near-future levels of temperature and pCO_2 reduce coral fertilization success. PLoS One **8**: e56468. doi:10.1371/journal.pone.0056468

Anderson, M. J. 2005. PERMANOVA: A FORTRAN computer program for permutational multivariate analysis of variance. Department of Statistics, Univ. of Auckland.

Baggini, C., M. Salomidi, E. Voutsinas, L. Bray, E. Krasakopoulou, and J. M. Hall-Spencer. 2014. Seasonality affects macroalgal community response to increases in pCO_2. PLoS One **9**: e106520. doi:10.1371/journal.pone.0106520

Bak, R. P. M., and E. H. Meesters. 1998. Coral population structure: The hidden information of colony size-frequency distributions. Mar. Ecol. Prog. Ser. **162**: 301 306. doi: 10.3354/meps162301

Brading, P., M. E. Warner, P. Davey, D. J. Smith, E. P. Achterberg, and D. J. Suggett. 2011. Differential effects of ocean acidification on growth and photosynthesis among phylotypes of *Symbiodinium* (Dinophyceae). Limnol. Oceanogr. **56**: 927 938. doi:10.4319/lo.2011.56.3.0927

Bramanti, L., M. Iannelli, T. Y. Fan, and P. J. Edmunds. 2015. Using demographic models to project the effects of climate change on scleractinian corals: *Pocillopora damicornis* as a case study. Coral Reefs **34**: 505 515. doi:10.1007/s00338-015-1269-z

Caldeira, K., and M. E. Wickett. 2003. Anthropogenic carbon and ocean pH. Nature **425**: 365 365. doi:10.1038/425365a

Capaccioni, B., F. Tassi, D. Vaselli, D. Tedesco, and R. Poreda. 2007. Submarine gas burst at Panarea Island (southern Italy) on 3 November 2002: A magmatic versus hydrothermal episode. J. Geophys. Res. **112**: B05201. doi:10.1029/2006JB004359

Caroselli, E., G. Falini, S. Goffredo, Z. Dubinsky, and O. Levy. 2015. Negative response of photosynthesis to natural and projected high seawater temperatures estimated by pulse amplitude modulation fluorometry in a temperate coral. Front. Physiol. **6**: 317. doi:10.3389/fphys.2015.00317

Caroselli, E., F. Ricci, V. Brambilla, G. Mattioli, O. Levy, G. Falini, Z. Dubinsky, and S. Goffredo. 2016. Relationships between growth, population dynamics, and environmental parameters in the solitary non-zooxanthellate scleractinian coral *Caryophyllia inornata* along a latitudinal gradient in the Mediterranean Sea. Coral Reefs **35**: 507 519. doi: 10.1007/s00338-015-1393-9

Caroselli, E., and others. 2017. Growth, population dynamics and reproductive output model of the non-zooxanthellate temperate solitary coral *Caryophyllia inornata* (Scleractinia, Caryophylliidae). Limnol. Oceanogr. **3**: 1111 1121. doi: 10.1002/lno.10489

De Astis, G., G. Ventura, and G. Vilardo. 2003. Geodynamic significance of the Aeolian volcanism (Southern Tyrrhenian Sea, Italy) in light of structural, seismological, and geochemical data. Tectonics **22**: 1040. doi:10.1029/2003TC001506

Doropoulos, C., S. Ward, G. Diaz-Pulido, O. Hoegh-Guldberg, and P. J. Mumby. 2012. Ocean acidification reduces coral recruitment by disrupting intimate larval-algal settlement interactions. Ecol. Lett. **15**: 338 346. doi:10.1111/j.1461-0248.2012.01743.x

Dufault, A. M., V. R. Cumbo, T.-Y. Fan, and P. J. Edmunds. 2012. Effects of diurnally oscillating pCO_2 on the calcification and survival of coral recruits. Proc. R. Soc. Lond. Ser. B Biol. Sci. doi:10.1098/rspb.2011.2545

Fabricius, K. E., and others. 2011. Losers and winners in coral reefs acclimatized to elevated carbon dioxide concentrations. Nat. Clim. Chang. **1**: 165 169. doi:10.1038/nclimate1122 Fabricius, K. E., S. H. C. Noonan, D. Abrego, L. Harrington, and G. De'ath. 2017. Low recruitment due to altered settlement substrata as primary constraint for coral communities under ocean acidification. Proc. R. Soc. B **284**: 20171536. doi:10.1098/rspb.2017.1536

Fantazzini, P., and others. 2015. Gains and losses of coral skeletal porosity changes with ocean acidification acclimation. Nat. Commun. **6**: 7785. doi:10.1038/ncomms8785

Gamberi, F., P. M. Marani, and C. Savelli. 1997. Tectonic, volcanic and hydrothermal features of submarine portion of Aeolian arc (Tyrrhenian Sea). Mar. Geol. **140**: 167 181. doi:10.1016/S0025-3227(97)00020-0

Gizzi, F., L. de Mas, V. Airi, E. Caroselli, F. Prada, G. Falini, Z. Dubinsky, and S. Goffredo. 2017. Reproduction of an azooxanthellate coral is unaffected by ocean acidification. Sci. Rep. **7**: 13049. doi:10.1038/s41598-017-13393-1

Goffredo, S., S. Arnone, and F. Zaccanti. 2002. Sexual reproduction in the Mediterranean solitary coral *Balanophyllia europaea* (Scleractinia, Dendrophylliidae). Mar. Ecol. Prog. Ser. **229**: 83 94. doi:10.3354/meps229083

Goffredo, S., L. Mezzomonaco, and F. Zaccanti. 2004. Genetic differentiation among populations of the Mediterranean hermaphroditic brooding coral *Balanophyllia europaea* (Scleractinia: Dendrophylliidae). Mar. Biol. **145**: 1075 1083. doi:10.1007/s00227-004-1403-x

Goffredo, S., E. Caroselli, E. Pignotti, G. Mattioli, and F. Zaccanti. 2007. Variation in biometry and population density of solitary corals with environmental factors in the Mediterranean Sea. Mar. Biol. **152**: 351 361. doi:10.1007/s00227-007-0695-z

Goffredo, S., E. Caroselli, G. Mattioli, E. Pignotti, and F. Zaccanti. 2008. Relationships between growth, population structure and sea surface temperature in the temperate solitary coral *Balanophyllia europaea* (Scleractinia, Dendrophylliidae). Coral Reefs **27**: 623 632. doi:10.1007/s00338-008-0362-y

Goffredo, S., E. Caroselli, G. Mattioli, E. Pignotti, Z. Dubinsky, and F. Zaccanti. 2009. Inferred level of calcification decreases along an increasing temperature gradient in a Mediterranean endemic coral. Limnol. Oceanogr. **54**: 930 937. doi:10.4319/lo.2009.54.3.0930

Goffredo, S., E. Caroselli, G. Mattioli, and F. Zaccanti. 2010. Growth and population dynamic model for the non-zooxanthellate temperate solitary coral *Leptopsammia pruvoti* (Scleractinia, Dendrophylliidae). Mar. Biol. **157**: 2603 2612. doi:10.1007/s00227-010-1522-5

Goffredo, S., and others. 2014. Biomineralization control related to population density under ocean acidification. Nat. Clim. Chang. **4**: 593 597. doi:10.1038/nclimate2241

Hall-Spencer, J. M., and others. 2008. Volcanic carbon dioxide vents show ecosystem effects of ocean acidification. Nature **454**: 96 99. doi:10.1038/nature07051

Hoegh-Guldberg, O., E. S. Poloczanska, W. Skirving, and S. Dove. 2017. Coral reef ecosystems under climate change and ocean acidification. Front. Mar. Sci. **4**: 158. doi: 10.3389/fmars.2017.00158

Inoue, S., H. Kayanne, S. Yamamoto, and H. Kurihara. 2013. Spatial community shift from hard to soft corals in acidified water. Nat. Clim. Chang. **3**: 683 687. doi:10.1038/nclimate1855

Johnson, M. D., V. W. Moriarty, and R. C. Carpenter. 2014. Acclimatization of the crustose coralline alga *Porolithon onkodes* to variable pCO_2. PLoS One **9**: e87678. doi:10.1371/journal.pone.0087678

Johnson, V. R., B. D. Russell, K. E. Fabricius, C. Brownlee, and J. M. Hall-Spencer. 2012. Temperate and tropical brown macroalgae thrive, despite decalcification, along natural CO_2 gradients. Glob. Chang. Biol. **18**: 2792 2803. doi:10.1111/j.1365-2486.2012.02716.x

Jokiel, P. L., K. S. Rodgers, I. B. Kuffner, A. J. Andersson, E. F. Cox, and F. T. Mackenzie. 2008. Ocean acidification and calcifying reef organisms: A mesocosm investigation. Coral Reefs **27**: 473 483. doi:10.1007/s00338-008-0380-9

Kerrison, P., J. M. Hall-Spencer, D. J. Suggett, L. J. Hepburn, and M. Steinke. 2011. Assessment of pH variability at a coastal CO_2 vent for ocean acidification studies. Estuar. Coast. Shelf Sci. **94**: 129 137. doi:10.1016/j.ecss.2011.05.025

Knittweis, L., J. Jompa, C. Richter, and M. Wolff. 2009. Population dynamics of the mushroom coral *Heliofungia actiniformis* in the Spermonde Archipelago, South Sulawesi, Indonesia. Coral Reefs **28**: 793 804. doi:10.1007/s00338-009-0513-9

Kroeker, K. J., R. L. Kordas, R. Crim, I. E. Hendriks, L. Ramajo, G. S. Singh, C. M. Duarte, and J. P. Gattuso. 2013. Impacts of ocean acidification on marine organisms: Quantifying sensitivities and interaction with warming. Glob. Chang. Biol. **19**: 1884 1896. doi:10.1111/gcb.12179

Linares, C., and others. 2015. Persistent natural acidification drives major distribution shifts in marine benthic ecosystems. Proc. R. Soc. Lond. Ser. B Biol. Sci. **282**: 20150587. doi:10.1098/rspb.2015.0587

Medina-Rosas, P., A. M. Szmant, and R. F. Whitehead. 2012. CO_2 enrichment and reduced seawater pH had no effect on the embryonic development of *Acropora palmata* (Anthozoa, Scleractinia). Invertebr. Reprod. Dev. **57**: 132 141. doi:10.1080/07924259.2012.704407

Morita, M., R. Suwa, A. Iguchi, M. Nakamura, K. Shimada, K. Sakai, and A. Suzuki. 2009. Ocean acidification reduces sperm flagellar motility in broadcast spawning reef invertebrates. Zygote **18**: 103 107. doi:10.1017/S0967199409990177

Nakamura, M., S. Ohki, A. Suzuki, and K. Sakai. 2011. Coral larvae under ocean acidification: Survival, metabolism, and metamorphosis. PLoS One **6**: e14521. doi:10.1371/journal.pone.0014521

Nakamura, M., and M. Morita. 2012. Sperm motility of the scleractinian coral *Acropora digitifera* under preindustrial,

current, and predicted ocean acidification regimes. Aquat. Biol. **15**: 299 302. doi:10.3354/ab00436

Prada, F., and others. 2017. Ocean warming and acidification synergistically increase coral mortality. Sci. Rep. **7**: 40842. doi:10.1038/srep40842

Rodolfo-Metalpa, R., and others. 2011. Coral and mollusc resistance to ocean acidification adversely affected by warming. Nat. Clim. Chang. **1**: 308 312. doi:10.1038/nclimate1200

Stocker, T. F., and others. 2013. Technical summary, p. 33 115. *In* T. F. Stocker, and others [eds.], Climate Change 2013: The physical science basis contribution of working group I to the fifth assessment report of the Intergovernmental Panel on Climate Change. Cambridge Univ. Press.

Tassi, F., and others. 2009. Low-pH waters discharging from submarine vents at Panarea Island (Aeolian Islands, southern Italy) after the 2002 gas blast: Origin of hydrothermal fluids and implications for volcanic surveillance. Appl. Geochem. **24**: 246 254. doi:10.1016/j.apgeochem.2008.11.015

Vizzini, S., R. Di Leonardo, V. Costa, C. D. Tramati, F. Luzzu, and A. Mazzola. 2013. Trace element bias in the use of CO_2 vents as analogues for low pH environments: Implications for contamination levels in acidified oceans. Estuar. Coast. Shelf Sci. **134**: 19 30. doi:10.1016/j.ecss.2013.09.015

Webster, N. S., S. Uthicke, E. S. Botté, F. Flores, and A. P. Negri. 2013. Ocean acidification reduces induction of coral settlement by crustose coralline algae. Glob. Chang. Biol. **19**: 303 315. doi:10.1111/gcb.12008

Acknowledgments

Ilana Berman Frank helped with alkalinity measurements. Bartolo Basile, Francesco Sesso, and Eolo Sub diving center assisted in the field. The Scientific Diving School supplied scientific, technical, and logistical support. The experiments comply with current Italian law. This study is in memory of Prof. Bruno Capaccioni. This research was funded by the ERC under the EU FP7 grant agreement n° (249930 CoralWarm: Corals and global warming: the Mediterranean vs. the Red Sea). EC was supported by the ALMA IDEA grant of the University of Bologna for the project "STRAMICRO." The authors declare no competing financial interests. All data are available from the corresponding author upon request.

Conflict of Interest

None declared.